Journal of the Korean Chemical Society
2023, *Vol. 67, No. 3*
Printed in the Republic of Korea
https://doi.org/10.5012/jkcs.2023.67.3.204

Note

Density Functional Theory Study on *β*-Hydrogen Elimination Reaction at a PPC Nickel Complex

Yongseong Kim, Joon Hyub Kim[†], Seung Soon Jang[‡], and Sungu Hwang[†,*]

Department of Pharmaceutical Engineering, Kyungnam University, Changwon 51767, Korea.
[†]Department of Nanomechatronics Engineering, Pusan National University, Miryang 50463, Korea.
**E-mail: sungu@pusan.ac.kr*
[‡]School of Materials Science and Engineering, Georgia Institute of Technology, Atlanta, Georgia 30332, United States.
(Received March 28, 2023; Accepted May 5, 2023)

Key words: DFT, *β*-hydrogen elimination, Ni complex, PPC ligand, Heteroatom-containing ligand

Ni-alkoxy, Ni-thiolate, and Ni-amido complexes are important analog of Ni-alkyl complexes. These compounds are useful intermediates of the catalytic cycles for ethers, sulfides and amine production.[1] β-Hydrogen elimination reactions are considered side reactions that compete with important reactions, such as reductive elimination reaction, which results in C–X coupling, where X = C, N, or O or other hetero elements. On the other hand, the β-hydrogen elimination reaction is an important step in the hydrolysis of ether, i.e., the C–O bond cleavage reaction.[2]

Tridentate pincer ligands have been used as a model frame to explore many important organometallic reactions for more than forty years because they provide a planar arrangement of the ligand atoms around the central metal and rigid frameworks that reduce the conformational complexity.[3] Typical tridentate pincer ligands are symmetric, i.e., two P atoms at both ends and a C/N/O atom in the middle. With this type of ligand, organometallic reactions occur between the substrates, and the pincer ligands of the complexes serve as the non-reacting rigid framework. A new type of tridentate pincer ligand, which has a non-symmetric arrangement of donor atoms, i.e., PPC pincer arrangement around the central transition metal atom, was recently reported.[4] (See *Scheme* 1)

With this nonsymmetrical type of pincer ligand, the boundary of the reaction could be extended to reactions between the substrate R_2 and the phenyl ring of the pincer ligand. A recent paper reported the results of density functional theory (DFT) studies on the reductive elimination and hydride transfer reactions between the alkyl substrate and the PPC ligand of Ni complexes.[5] The present work reports the results of a computational study on the alkoxy, thiolate, and amido complexes of Ni with the PPC ligand.

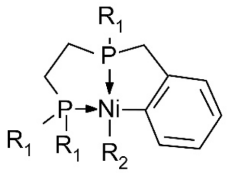

R_1 = Me, or ^{t}Bu, R_2 = alkyl, alkoxy, thiolate, or amido

***Scheme* 1.** Ni PPC pincer complexes.

Table 1 lists the Gibbs free energy of activation ($\Delta G^{\dagger}$) for reductive elimination and β-hydrogen transfer for various Ni complexes reported in Ref 4 and their analogs. Two reaction paths were considered. For β-hydrogen transfer from the substrate R_2 to the phenyl ring of the pincer ligand: Path 1) β-hydrogen elimination followed by C–H reductive elimination, and Path 2) σ-CAM mechanism as depicted in *Scheme* 2. Path 1 is the conventional pathway in which C=X double-bonded species do not participate directly in the second step of the path, and H is transferred from Ni to the recipient carbon atom. On the other hand, X, C, and H atoms are located in the same plane as the recipient carbon atom in path 2, and H is transferred from the carbon atom of the R_2 substrate to the phenyl ring. For general substrate dependence, the $\Delta G^{\dagger}$ for the β-hydrogen transfer reaction is in increasing order: alkoxy < imido < thiolate, which is in excellent agreement with the experimental observation.[4] The $\Delta G^{\dagger}$ for the reductive elimination reactions differs from the order for the β-hydrogen transfer, which also agrees with the experimental results for the late transition metal complexes with the bidentate ligands.[6] Complexes containing polarizable and nucleophilic thiolate ligands have faster reaction rates than complexes with alkoxy ligands. The only exception to the general trend is

***Table* 1.** Gibbs free energy of activation, $\Delta G^{\dagger}$, for the reactions at Ni center in PPC Ni complexes at B3PW91-d3/LACVP** level with continuum solvation model of tetrahydrofuran (in kcal mol^{-1})

R_2	β-H transfer, hydride path		
	R_1 = Me	R_1 = ^{i}Pr	R_1 = ^{t}Bu
O-^{i}Pr	30.1 (TS1)	30.5 (TS1)	33.5 (TS1)
	16.3 (TS2)	19.9 (TS2)	16.0 (TS2)
S-^{i}Pr	46.2 (TS1)	48.5 (TS1)	48.8 (TS1)
	34.9 (TS2)	40.3 (TS2)	38.9 (TS2)
NPhMe	39.9 (TS1)	38.3 (TS1)	35.5 (TS1)
	33.6 (TS2)	35.5 (TS2)	34.0 (TS2)
R_2	β-H transfer, σ-CAM path		
	R_1 = Me	R_1 = ^{i}Pr	R_1 = ^{t}Bu
O-^{i}Pr	35.2 (TS1)	38.9 (TS1)	34.8 (TS1)
	17.3 (TS2)	25.5 (TS2)	24.5 (TS2)
S-^{i}Pr	37.2 (TS1)	38.5 (TS1)	37.6 (TS1)
	24.5 (TS2)	29.5 (TS2)	28.2 (TS2)
NPhMe	40.7 (TS1)	45.2 (TS1)	48.1 (TS1)
	27.8 (TS2)	36.3 (TS2)	32.6(TS2)
R_2	Reductive elimination		
	R_1 = Me	R_1 = ^{i}Pr	R_1 = ^{t}Bu
O-^{i}Pr	42.1	42.9	41.0
S-^{i}Pr	39.9	40.1	40.5
NPhMe	40.6	39.9	35.7

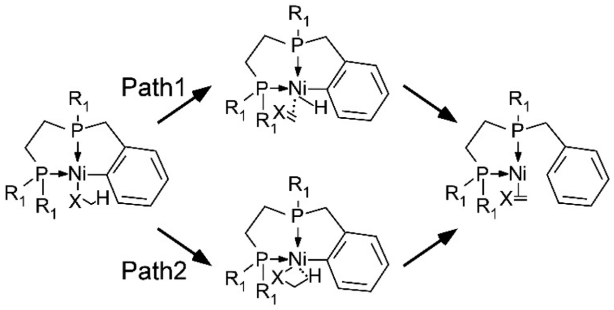

***Scheme* 2.** Two β-hydrogen transfer pathways.

the case of large alkyl substituents on P atoms with a large imido substrate where the steric effect in the reactant dominates.

For alkoxy substrate, the $\Delta G^{\dagger}$ for the β-hydrogen transfer is much smaller than that for the reductive elimination, which is consistent with the experimental result.[4] The β-H elimination followed by the aryl-H reductive elimination pathway is slightly favored over the σ-CAM, which is similar to the previous experimental result with Ni PCP complex.[2] The dependence on the substituent of the P atoms is relatively small compared to rigid, symmetric tridentate cases studied previously.[7] Ni PCP pincer complexes with higher alkoxy ligands are thermally very stable and only undergo β-hydrogen elimination slowly at high temperatures around 100 ℃,[8] which is in sharp contrast to the present study with an asymmetric and flexible PPC ligand.

For the imido substrate, the $\Delta G^{\dagger}$ for the H transfer reaction and the reductive elimination reaction are comparable. Unlike other substrates, the large size of the substrate destabilizes the reactant with ^{t}Bu-substituted PPC ligand, resulting in relatively smaller $\Delta G^{\dagger}$ than Me- and iPr-substituted PPC ligands. The calculated $\Delta G^{\dagger}$ for the imido substrate is slightly larger than the alkoxy substrate, which agrees with the experimental observations.[4]

For the S^{i}Pr substrate, the σ-CAM route of the H transfer has a lower $\Delta G^{\dagger}$ than the hydride route of H transfer and reductive elimination reactions, as shown in *Table* 1. For bidentate Pd DPPE complexes, C–S coupling via reductive elimination is expected,[1] in which S^{t}Bu is coupled to toluene over the temperature range of 40–70 ℃ with the activation Helmholtz free energy $\Delta H^{\ddagger}$ of 25.2 kcal mol^{-1}. Rapid equilibrium exists for Ar/SAr' and Ar'/SAr ligands for bidentate Ni complex at room temperature, which suggests that the reductive elimination followed by the oxidative addition reaction of the C–S bond occurs at room temperature.[9] Nevertheless, the thiolate substrate with PPC tridentate ligand in this study has the highest $\Delta G^{\dagger}$ compared to the other substrates, which agrees with the experimental results.[4]

The computed geometries cannot be compared with the experimental ones directly because the PPC Ni oxo complexes in this study are reactive. On the other hand, the geometries of PCP Ni oxo complexes were reported previously. The Ni–O and O–C distances of the complex R_1 = ^{t}Bu and R_2 = O^{i}Pr in this study were calculated to be 1.90 Å and 1.40 Å, respectively, which is in excellent agreement with the geometries found in PCP Ni complexes.[8] Regarding the NMePh substrate that is not reactive at room temperature, RMS deviation from the experiments is 0.17 Å (all heavy atoms) and 0.05 Å (pincer chain). The calculated Ni–N distance of 1.94 Å is in excellent agreement with the experiment[4] and slightly larger than similar NH_2 complexes with a PCP pincer ligand.[10] RMS deviation from the experimental X-ray structure for the thiolate substrate is 0.17 Å (all heavy atoms) and 0.06 Å (pincer chain). The main deviations are located on the ^{t}Bu side chains on P atoms, which may be subjected to the crystal packing constraints. The calculated Ni–S distance of 2.29 Å is in excellent agreement with the experimental X-ray structures in Ni-PPC,[4] Ni-PCP,[11] and Ni-PNP[12] thiolate complexes.

Fig. 1 presents the geometry of the TS's of β-H transfer reaction in path 1 for the PPC oxo complex (R_1 = ^{t}Bu, R_2 = O-^{i}Pr). In the TS of the first step, the Ni–O bond is almost bro-

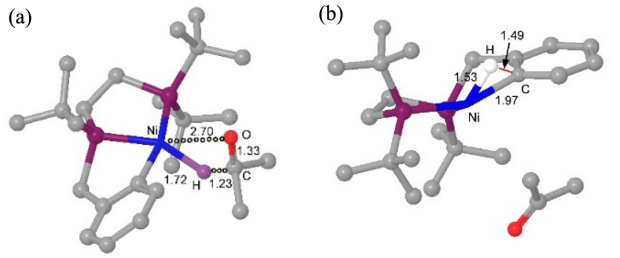

***Figure* 1.** Geometry of the transition states in the β-H elimination route for Ni PPC oxo complex: (a) the first step and (b) the second step.

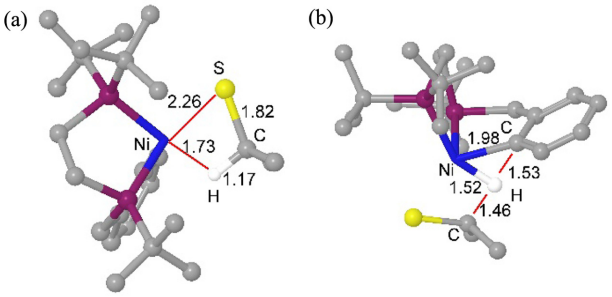

***Figure* 2.** Geometry of the transition states in the σ-CAM route for Ni PPC thiolate complex: (a) the first step and (b) the second step.

ken with a large distance, and the H atom is in the course of transfer from C to Ni. In the second step, the H atom is transferred from Ni to C of the phenyl ring of the ligand. The dissociated ketone in the first step does not participate in the transfer process.

For the S^{i}Pr substrate, the σ-CAM route has a lower $\Delta G^{\dagger}$ than the hydride route, as shown in *Table* 1. *Fig.* 2 is the geometry of the transition states for the σ-CAM route. Unlike the oxo complexes, the thiolate substrate involves in the H transfer process, and Ni, S, C (thiolate), H, and C (phenyl) atoms are located in the same plane, as shown in *Fig.* 2(b).

For an amido ligand with an α-hydrogen, it is also possible to have an α hydrogen transfer reaction that would result in a Ni imido complex. *Table* 2 lists the $\Delta G^{\dagger}$ of the reaction for the NHiPr substrate. α abstraction leading to metal-carbene complexes has the highest activation barrier for all the cases, and β-H transfer via the σ-CAM route and reductive elimination show comparable activation barriers. Steric or electronic effects due to side chains on the ligand phosphorus atoms were barely found for all three reactions, which was also found for the other Ni pincer complexes in this study.

In conclusion, DFT computational methods were used to study various reactions at the transition metal center of

***Table* 2.** Gibbs free energy of activation, $\Delta G^{\dagger}$, for the reactions at Ni center in PPC Ni–NH^{i}Pr complexes at B3PW91-d3/LACVP** level with continuum solvation model of tetrahydrofuran. (in kcal mol^{-1})

Ligand R_2 = NH^{i}Pr	B3PW91-d3		
	R_1 = Me	R_1 = ^{i}Pr	R_1 = ^{t}Bu
α abstraction	53.3	53.0	51.4
β-H transfer	38.8 (TS1)	40.9(TS1)	41.6 (TS1)
hydride pathway	13.5 (TS2)	14.9 (TS2)	10.1 (TS2)
β-H transfer	29.6 (TS1)	32.1 (TS1)	28.1 (TS1)
σ-CAM pathway	13.9 (TS2)	20.9 (TS2)	17.2 (TS2)
Reductive elimination	32.1	31.2	28.2

PPC Ni complexes. The computational results were in excellent agreement with the experiments. The alkoxy complexes show facile reactivity and thiolate complexes are the least reactive. For the amido ligands with an α-hydrogen, α abstraction has the highest activation barrier, which indicates that Ni imido complex is not obtained in this synthetic route.

COMPUTATIONAL DETAILS

The geometry of the chemically relevant structures, i.e., minima and maxima along the reaction coordinates of the various reactions, such as reductive elimination, *α* abstraction, and β elimination considered in this work, were optimized using the Jaguar v8.8 suite.[13] The functional and the basis set for DFT adopted in the present study was B3PW91-d3/LACVP**, which shows excellent agreement with the experimental data for the pincer transition metal complexes by considering van der Waals interactions.[14] Harmonic vibrational frequency calculations were performed to identify all the optimized structures by counting the number of imaginary frequencies and calculating the thermodynamic quantities at 298 K under 1 bar pressure through rigid rotor-harmonic oscillator approximation. Intrinsic reaction coordinate calculations were also performed to verify the reaction paths from the transition states to the minima of the reaction paths (the reactant, the intermediate, or the product).[15,16]

Acknowledgments. This work was supported by a 2-Year Research Grant of Pusan National University.

REFERENCES

1. Mann, G.; Baranano, D.; Hartwig, J. F.; Rheingold, A. L.; Guzei, I. A. *J. Am. Chem. Soc.* **1998**, *120*, 9205.

2. Kelley, P.; Lin, S.; Edouard, G.; Michael, W.; Day, M. W.; Agapie, T. *J. Am. Chem. Soc*. **2012**, *134*, 5480
3. Martínez-Prieto, L. M.; Ávila, E.; Palma P.; Álvarez, E.; Cámpora, J. *Chem. Eur. J.* **2015**, *21*, 9833
4. Zimmerman, A. C.; Fryzuk, M. D. *Organometallics* **2018**, *37*, 2305.
5. Kim, Y.; Cho, H.; Hwang, S. *Bull. Korean Chem. Soc.* **2022**, *43*, 784
6. Hartwig, J. F. *Nature* **2008**, *455*, 314.
7. Kim, Y.; Ryu, S.-C.; Hwang, S. *Bull. Korean Chem. Soc.* **2019**, *40*, 189.
8. Martínez-Prieto, Palma P.; Álvarez, E.; Cámpora, J. *Inorg. Chem.* **2017**, *56*, 13086.
9. Osakada, K.; Maeda, M.; Nakamura, Y.; Yamamoto, T.; Yamamoto, A. *J. Chem. Soc. Chem. Commun.* **1986**, 442.
10. Cámpora, J.; Palma P.; del Río, D.; Conejo, M. M.; Álvarez, E. *Organometallics* **2004**, *24*, 5653.
11. Kaur-Ghumaan, S.; Hashe, P.; Spannenberg, A.; Beweries, T. *Dalton Trans.* **2019**, *48*, 16322.
12. van der Vlugt, J. I.; Lutz, M.; Pidko, E. A.; Vogt, D.; Spek, A. L. *Dalton Trans.* **2009**, *38*, 1016.
13. Jaguar, v8.8 Schrodinger Inc.: New York, NY 2015.
14. Gu, S.; Nielsen, R. J.; Taylor, K. H.; Fortman, G. C.; Chen, J.; Dickie, D. A.; Goddard III, W. A.; Gunnoe, T. B. *Organometallics* **2020**, *39*, 1917.
15. Gonzalez, C.; Schlegel, H. B. *J. Chem. Phys.* **1989**, *90*, 2154.
16. Gonzalez, C.; Schlegel, H. B. *J. Phys. Chem.* **1990**, 94, *55*23.